JACS
JOURNAL OF THE AMERICAN CHEMICAL SOCIETY
pubs.acs.org/JACS

Article

Revealing the Full Potential of Glycolated Mixed Ionic-Electronic Semiconductors – Symmetric Monomer Polymerization to Boost Electrochemical Transistor Performance

Lize Bynens,◆ Paola Mantegazza,◆ Adam Marks, Yeongmin Park, Arwin Goossens, Stefania Moro, Tyler J. Quill, Garrett Lecroy, Christina Cheng, Arianna Magni, Laurence Lutsen, Jochen Vanderspikken,* Simon E. F. Spencer, Koen Vandewal, Alberto Salleo, Giovanni Costantini,* and Wouter Maes*

Cite This: J. Am. Chem. Soc. 2026, 148, 8383–8392

Read Online

ACCESS | Metrics & More | Article Recommendations | Supporting Information

ABSTRACT: Organic electrochemical transistors (OECTs) enable the transduction of ionic signals into electronic outputs, positioning them as ideal candidates for next-generation sensing and (bio)signal processing applications. Recent years have witnessed the development of various OECT channel materials, affording insights into structural fine-tuning to achieve optimal performance and/or stability. However, homocouplings, commonly present in alternating conjugated polymers, have largely been overlooked. This study investigates the effect of homocoupling on OECT materials by employing two synthesis methods – standard Stille polymerization and an alternative symmetric approach – to create the p-type enhancement-mode benchmark polymer pgBTTT. The impact of homocoupling, and its absence, is studied by comparing the bulk properties of the two polymers and evaluating their respective OECT metrics. The new, homocoupling-free polymer exhibits a notably improved OECT performance (μC^*), mainly due to an average 3-fold increase in electronic mobility (μ).

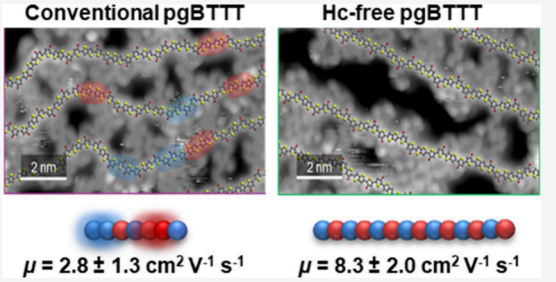

INTRODUCTION

State-of-the-art alternating semiconducting copolymers are traditionally synthesized via established cross-coupling protocols such as Stille and Suzuki polymerization.[1−3] The resulting alternating structure is most often simply assumed based on the flawless selectivity of the two complementary functionalized comonomers. In practice, however, two identical monomers can react instead, producing homocoupling defects. This causes the obtained structure to deviate from the perfectly alternating one.[4−8] Since the occurrence of homocoupling depends on many factors and does not appear consistently, these structural defects hamper the reproducibility across different polymer batches, posing a challenge to the commercial viability of polymeric semiconductor applications. Furthermore, homocoupling defects may induce performance limitations,[1] as shown for organic photovoltaics and photodetectors.[5,9−14]

The occurrence and impact of structural defects in organic electrochemical transistor (OECT) materials remain largely unexplored. OECTs have garnered significant attention due to their exceptional sensitivity and selectivity, coupled with their compatibility with soft and flexible substrates.[15] These devices offer a unique interface between ionic and electronic conductors, enabling the transduction of ionic (bio)signals into electronic outputs.[16] Significant efforts have been directed at increasing the performance of p-type OECTs in enhancement-mode, where the application of a gate potential is required to dope the channel material with positive electronic charge carriers (holes).[17,18] The enhancement-mode operation allows for a high transistor gain, low-power operation, and high sensitivity, making it a sought-after configuration for sensing applications.[19,20] In this context, the choice of an appropriate channel material plays a pivotal role in determining the overall device performance and operational characteristics.[21] Recent years have witnessed the development of many new, often intricate OECT channel materials.[21−28] Among these, glycolated organic mixed ionic-electronic conductors (OMIECs) have shown significant promise in achieving high performance in p-type OECTs because of their volumetric electrochemical charging capabilities.[17,22,24,25,29] However, studying performance-limiting morphological and structural

Received: October 28, 2025
Revised: February 10, 2026
Accepted: February 12, 2026
Published: February 23, 2026

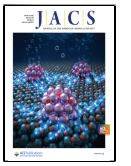

https://doi.org/10.1021/jacs.5c19024
J. Am. Chem. Soc. 2026, 148, 8383−8392

Scheme 1. Synthesis of Conventional and Homocoupling-Free pgBTTT[a]

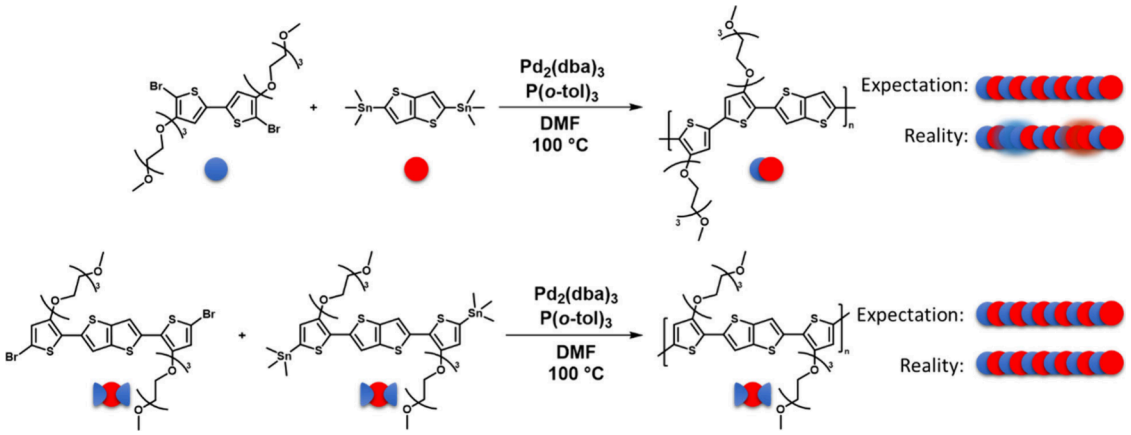

[a]Top: Reported synthesis route for pgBTTT,[33] employing a standard Stille polymerization, with a schematic representation of the homocoupling sequences that are introduced. Bottom: Symmetric Stille polymerization for homocoupling-free pgBTTT.

factors in these materials presents challenges due to the complex interplay between ionic and electronic charges within an OECT.[30,31] Computational modeling studies can contribute to our understanding but typically assume perfectly alternating polymer backbones, which may not accurately reflect experimentally realized materials.[11,32] As OECT performance continues to advance, attention should be directed toward the reproducibility and structural fidelity of these complex polymers. Structural defects can obscure structure−property relationships and hinder meaningful comparison between experimental and theoretical studies. It is therefore essential to ensure that the synthesized material precisely reflects its intended molecular structure in order to obtain reproducible device characteristics and accurate structure−property relationships.

To achieve a truly homocoupling-free polymer, alternative synthetic methods are required. Our study focuses on the homocoupling-free synthesis of the benchmark p-type enhancement-mode OECT material pgBTTT (poly[4,4′-bis(2-(2-(2-methoxyethoxy)ethoxy)ethoxy)-[2,2′-bithiophen]-5,5′-diyl]-*alt*-[thieno[3,2-*b*]thiophene-2,5-diyl]), first reported by Hallani et al.[33] pgBTTT consists of glycolated bithiophene (gBT) and unsubstituted thieno[3,2-*b*]thiophene (TT) units, which in theory should alternate regularly. The standard Stille polymerization employed in the synthesis of pgBTTT and numerous other semiconducting polymers involves coupling a distannylated monomer to a dibrominated one using a palladium (Pd) catalyst (Scheme 1).[1] This strategy is widely applied in academic settings because of its mild reaction conditions and the reasonably high molar masses it affords.[1] However, this polymerization route introduces homocoupling defects within the polymer backbone, as recently illustrated for alkoxy-substituted pBTTT analogs (Scheme S3).[11,34] While it is known that these side reactions occur and thus most OECT channel materials contain homocoupling defects, this aspect is generally disregarded when interpreting OECT results. On the other hand, molar mass has been established as a critical parameter with substantial influence on the performance of both p- and n-type OECTs.[35−39] For p-type OECTs, it has been reported that increasing the molar mass of the channel material enhances mobility and hence overall performance, up to a system-specific threshold, after which it decreases again.[38,39] However, different molar mass fractions may contain a different number of defects, adding to the uncertainty of which parameter truly determines performance.

To elucidate the impact of homocoupling defects in a benchmark OECT material, pgBTTT was synthesized both via the standard Stille polymerization and an alternative symmetric Stille route (Scheme 1, Scheme S4). In the symmetric monomer polymerization, any self-coupling between brominated or stannylated monomers still yields a perfectly alternating gBT-TT backbone, thereby eliminating homocoupling defects. Matrix-assisted laser desorption/ionization − time-of-flight mass spectrometry (MALDI-ToF MS) and electrospray deposition − scanning tunneling microscopy (ESD-STM) were used to establish the structural integrity and the molar mass distributions of the polymers. We assess the influence of homocoupling defects on device performance by comparing the performance of both OMIECs in OECTs. It was found that the symmetric polymerization yields a polymer with a significantly increased performance (μC^*) compared to conventionally synthesized pgBTTT.

The symmetric Stille polymerization was found to completely avoid homocoupling while simultaneously yielding polymers of higher molar mass. Thus, this approach provides structurally well-defined materials, while also offering access to previously unachieved molar masses under identical reaction conditions. We therefore expect that it will contribute to more reproducible devices and more meaningful comparison with theoretical models. Together, these advances allow a more rigorous evaluation of how molecular precision and macromolecular properties govern charge transport in high-performance p-type OECTs.

RESULTS AND DISCUSSION

Conventional pgBTTT was synthesized according to a literature procedure (see Supporting Information, SI).[33] For the synthesis of homocoupling-free pgBTTT, different methods were explored. Ultimately, a symmetric, extended monomer was designed consisting of a thieno[3,2-*b*]thiophene core flanked by glycolated thiophenes, to avoid the possibility of TT and gBT homocouplings. While symmetric polymerization has been applied before using oxidative conditions,[11,40−42] this was scarcely successful here with glycolated monomers, and substantial synthetic optimization was hence required, as detailed in the SI (Section 2.3). It was found that

https://doi.org/10.1021/jacs.5c19024
J. Am. Chem. Soc. 2026, 148, 8383−8392

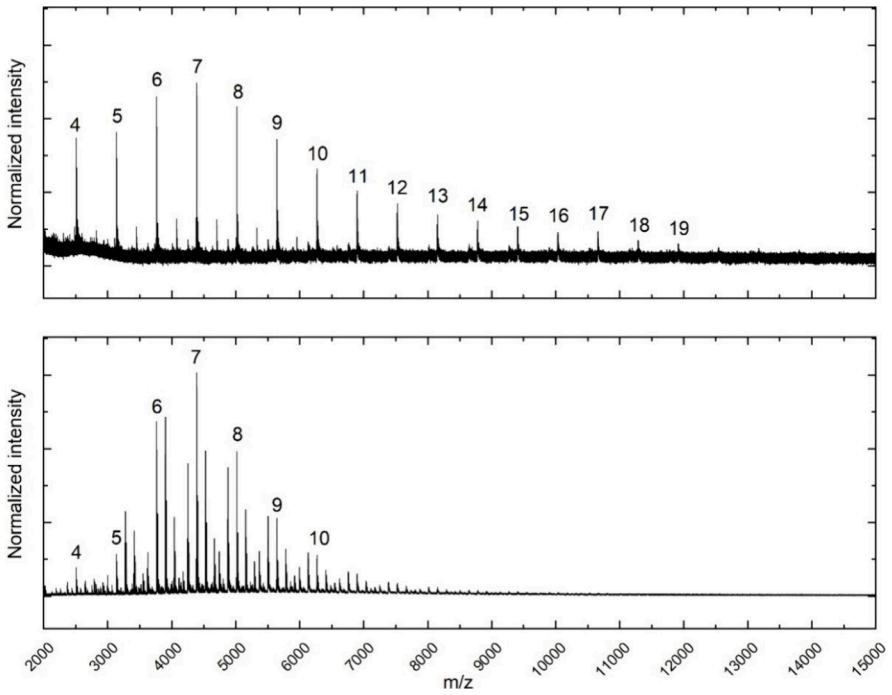

Figure 1. MALDI-ToF mass spectra (m/z range from 2 to 15 kDa) for homocoupling-free pgBTTT (top) and conventional pgBTTT (bottom). The chains containing a 1:1 ratio of gBT:TT units are indicated with their number (n) of 'gBTTT' repeat units above the respective peaks.

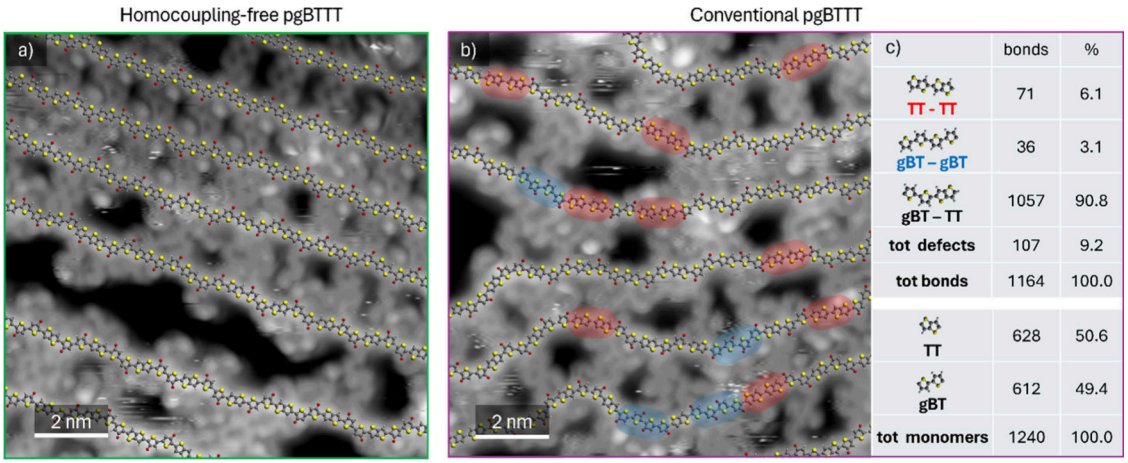

Figure 2. Examples of STM images of pgBTTT on a Au(111) surface, synthesized by a) symmetric Stille and b) standard Stille polymerization. Molecular models of the backbones are overlapped onto the experimental images and the different types of homocoupling defects (double thienothiophene, TT, or double glycolated bithiophene, gBT) are highlighted in red and blue, respectively. The defect frequencies observed in conventional pgBTTT are shown in c).

symmetric polymerization via Stille affords the best results, namely a high molar mass and homocoupling-free batch of pgBTTT (as obtained from the chloroform Soxhlet fraction). For this synthetic route, one portion of the symmetric monomer was brominated, while the other part was stannylated. Subsequent Stille polymerization can therefore only result in the target structure (Scheme 1), regardless of whether homocoupling occurs or not. Details of the monomer and polymer syntheses can be found in the SI. ^{1}H NMR spectra of the two polymers (Figure S4) look very similar, illustrating that the sensitivity of NMR is not sufficient to assess subtle structural differences, in particular under the employed experimental conditions ($CDCl_3$, room temperature), for which aggregation of the pgBTTT chains further broadens spectral features.

UV−vis-NIR absorption spectroscopy was conducted on films of conventional and homocoupling-free pgBTTT, revealing that homocoupling sequences do not significantly affect the absorption spectrum (Figure S15). To probe some of the electrochemical properties, cyclic voltammetry measurements were performed. The absence of homocoupling does not appear to have a notable impact on the frontier molecular orbital energy levels (HOMO and LUMO) or on the oxidation onsets (Table S2). The aqueous voltammograms (Figure S16, S17) are similar to each other and to the originally reported result for pgBTTT.[33]

To gain deeper insights into the polymer structures, MALDI-ToF MS analysis was performed (Figure 1). As expected, conventional pgBTTT displays numerous signals representing differing gBT:TT ratios. On the contrary,

https://doi.org/10.1021/jacs.5c19024
J. Am. Chem. Soc. 2026, 148, 8383−8392

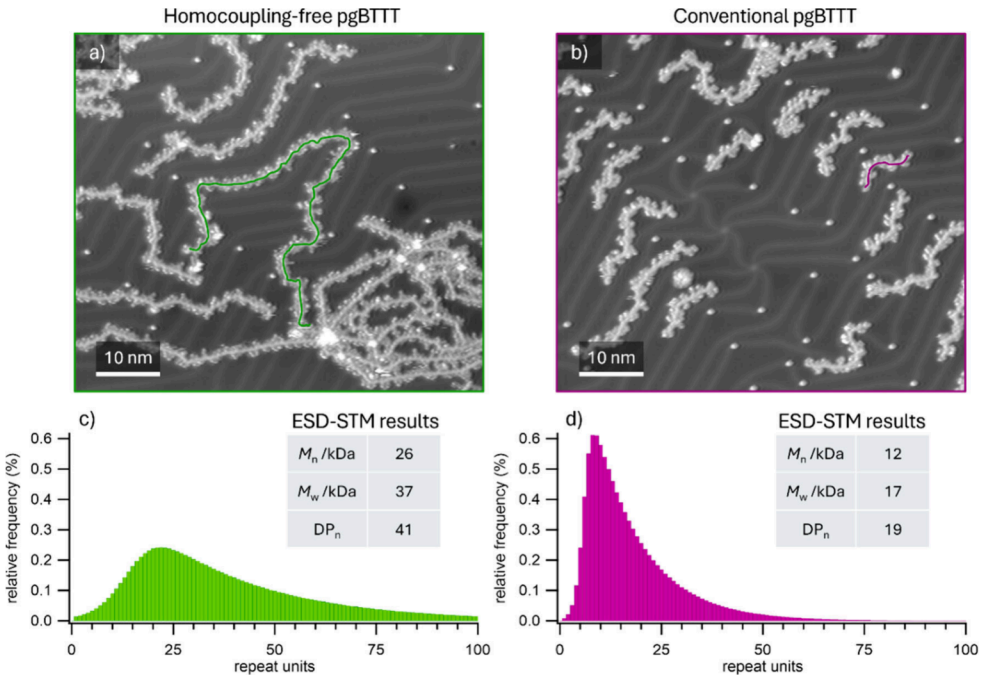

Figure 3. Examples of typical larger-scale STM images of a) symmetric Stille pgBTTT and b) conventional pgBTTT, used to construct the mass distributions. The lengths of the exemplary polymer profiles highlighted by colored lines in each image are 78 nm in a) and 11 nm in b), respectively. Experimental ESD-STM mass distributions (corrected by survival analysis, see SI) of c) symmetric Stille pgBTTT and d) conventional pgBTTT, alongside the values obtained for the statistical parameters M_n, M_w, and DP_n (using the same gBTTT repeat unit for both polymers).

pgBTTT prepared by the alternative symmetric approach consists of only chains exhibiting the desired ratio. While this is a strong indication of the significant difference in homocoupling content between the two pgBTTT batches, MALDI-ToF MS does not allow a straightforward quantification of the defect ratio. ESD-STM was hence employed to verify this observation in a quantitative manner and ascertain the nature of these homocoupling defects.[11,43−47] Figure 2 compares the chloroform (Soxhlet) fractions of the symmetric (a) and conventional (b) Stille polymers as imaged by ESD-STM. For both polymers, highly resolved STM images clearly show linear backbones and side chains interdigitating with a different degree of overlap between them. The images were carefully analyzed and fitted with molecular dynamics optimized molecular models of the different comonomers to identify potential homocoupling defects in the backbones.[11,34,43−46] To account for the different synthesis protocols, models of the gT-TT-gT unit were used to fit homocoupling-free pgBTTT, while separated models for gBT and TT were employed for conventional pgBTTT. Importantly, no defects were detected in the symmetric Stille polymer, whereas over 9% of the monomer couplings in the conventional Stille batch were homocoupling defects. Statistics on the different types of homocoupling defects identified in this batch are presented in Figure 2c.

Another striking difference between the two polymers in the MALDI-ToF MS spectra (Figure 1) is that homocoupling-free pgBTTT shows chains of higher molar mass. Thus, from the MS data it seems that the symmetric Stille polymerization delivers a polymer containing only chains with the desired 1:1 ratio of gBT and TT units and with a higher molar mass, using the same reaction conditions as applied for the standard Stille polymerization. Attempts to confirm the molar mass difference between the two polymers using gel permeation chromatography (GPC) in chloroform, chlorobenzene, or *N*,*N*-dimethylformamide were unsuccessful because the obtained GPC traces were either too broad or very low in intensity. This issue, caused by polymer aggregation or solubility issues in common GPC solvents, has been previously reported for glycolated polymers and frequently leads to an overestimation of the molar masses of these materials.[48−50] Recently, several studies have omitted GPC for the molar mass determination of such polymers, using alternative techniques like MALDI-ToF MS instead.[24,31] However, as previously noted, MALDI-ToF MS is not quantitative and can indicate molar mass trends but does not provide precise values.[51] Currently, the only technique that accurately measures the exact number- or weight-average molar masses (M_n and M_w, respectively) and polymerization degrees (DP_n) of glycolated OMIECs, while also attaining the full mass distribution, is ESD-STM.[44]

Measuring the length of line profiles traced along the polymer backbones in STM images for a large number of polymers enables the collection of complete mass distributions.[44] Figure 3 shows representative STM images of low-coverage areas of homocoupling-free and conventional pgBTTT, where individual polymer profiles are clearly distinguishable. The corresponding STM-derived mass distributions, with relevant mass numbers, are displayed in Figure 3c,d. A detailed description of the length-profile acquisition and the process to obtain the mass distributions is provided in the SI (Section 6). The results clearly show a significant difference in the lengths of the polymers for the two batches, with homocoupling-free pgBTTT chains being (on average) significantly longer than the conventional Stille ones, quantitatively confirming the observations derived from MALDI-ToF MS.

The higher frequency of homocouplings and the lower mass observed in conventional pgBTTT, compared to homocoupling-free pgBTTT, could suggest that such defects inhibit polymer chain growth. To investigate whether the presence of

https://doi.org/10.1021/jacs.5c19024
J. Am. Chem. Soc. 2026, 148, 8383−8392

Table 1. Summary of OECT Performance Parameters for Conventional pgBTTT (Chloroform Fraction) and Homocoupling-Free (hc-Free) pgBTTT[f]

pgBTTT	Conventional	Hc-free DCM fraction	Hc-free Batch 1	Hc-free Batch 2	Hc-free Batch 3
					
μ (cm^2 V^{-1} s^{-1}) [a]	2.8 ± 1.3	3.2 ± 0.8	8.3 ± 2.0	6.7 ± 2.2	8.6 ± 1.6
C^* (F cm^{-3}) [b]	188 ± 10	191 ± 10	188 ± 6	207 ± 13	213 ± 18
$\mu \times C^*$ (F cm^{-1} V^{-1} s^{-1}) [c]	530 ± 240	610 ± 150	1550 ± 380	1390 ± 450	1830 ± 350
μC^* (F cm^{-1} V^{-1} s^{-1}) [d]	1020 ± 80	1390 ± 80	1940 ± 190	1820 ± 170	1790 ± 190
V_{TH} (V) [e]	−0.18	−0.23	−0.19	−0.18	−0.22

[a]Calculated by measuring the electronic charge carrier transit time while pulsing constant gate current. The data were collected using devices with L = 500, 200, and 100 μm. Reported uncertainties are one standard deviation, with n = 5 devices. An approximate 3-fold increase in μ is observed for homocoupling-free pgBTTT compared to conventional pgBTTT, calculated based on the average μ from batch 1, 2, and 3. [b]Independently determined by EIS. Reported uncertainties are one standard deviation, with n = 3−5 devices. [c]Calculated by multiplying the independently determined μ and C^* values. Reported uncertainties are one standard deviation. [d]Extracted from the relationship between the transconductance values measured in the linear regime and the operating parameters (drain voltages and channel dimensions) by linear regression. The coefficient of determination, R^2, was larger than 0.8 for all batches. For each material, the RMS error is reported, calculated by performing a linear regression, with n = 15 samples. [e]Extracted in the saturation regime (V_D = −0.5 V) of each device (n = 5) by fitting the $I_D^{1/2}$ vs V_G plots. [f]Three independent batches of hc-free pgBTTT (chloroform fraction) were evaluated to demonstrate the reproducibility of the symmetric polymerization. The lower-molar-mass DCM fraction of hc-free pgBTTT (batch 1) was additionally measured to disentangle the effects of molar mass and homocoupling defects.

homocoupling defects indeed affects, and in particular hinders, the growth of polymer chains in conventional pgBTTT, we examined whether defects are uniformly distributed along the polymer chains and whether shorter polymers exhibit a higher number of homocouplings. The precise polymer sequencing enabled by ESD-STM allowed us to conduct three statistical tests to assess potential correlations between: (i) consecutive defects along the backbone, (ii) defect density and polymer length, and (iii) defective bonds and polymer ends. Our detailed analysis (see SI) revealed no statistically significant correlations in any of these tests. These observations indicate that homocoupling defects do not locally suppress polymer growth through chain-specific or position-dependent mechanisms. While it should be noted that the samples analyzed by ESD-STM were not crude products directly obtained from the polymerization reaction but rather those subjected to Soxhlet extractions, it is difficult to envision how the Soxhlet extractions could have selectively removed polymer chains exhibiting such correlations. Within this context, our findings suggest that homocoupling defects are unlikely to play a primary role in limiting polymer growth during Stille polymerization through local, defect-induced mechanisms, thereby challenging commonly held assumptions.

At the same time, a distinct global effect of homocoupling defects must be considered. Our measurements indicate that the TT and the gBT homocoupling reactions occur with different frequencies (Figure 2), suggesting that one monomer type is consumed more rapidly than the other during polymerization. This generates an effective stoichiometric imbalance as the reaction proceeds, which can reduce the degree of polymerization, in a manner analogous to that described by the Carothers equation for systems with genuine stoichiometric imbalance. A quantitative evaluation of this effect is nontrivial but simple estimates based on generalizations of Carothers equation suggest that the observed difference in homocoupling frequencies (∼3%) is unlikely to account for the nearly 2-fold reduction in the DP_n observed experimentally (Figure 3). It should finally be noted that an additional Soxhlet solvent (dichloromethane, DCM) was applied for homocoupling-free pgBTTT, which aids in removing shorter polymer chains (SI, Section 2.3).

The impact of homocoupling defects on device performance was assessed by incorporating the polymers in OECT channels with various aspect ratios (Table 1, Figure 4, S22, S23). All transfer curves were measured in the linear regime to ensure stable operation at low charge carrier densities.[31] The product of the electronic mobility and volumetric capacitance (μC^*) was extracted from the transfer curves and used as the figure of merit. Since the ESD-STM data revealed a distinct molar mass difference, and higher molar mass is generally associated with improved OECT performance,[38,39] this factor has to be taken into account. When comparing the highest molar mass (chloroform) fractions of both conventional and homocoupling-free pgBTTT, the latter exhibited significantly better performance (μC^* = 1020 ± 80 F cm^{-1} V^{-1} s^{-1} vs 1940 ± 190 F cm^{-1} V^{-1} s^{-1}). To distinguish the effects of molar mass and structural defects, the lower molar mass (DCM) Soxhlet fraction of homocoupling-free pgBTTT was included in the comparison. MALDI-ToF MS analysis suggests that the DCM fraction of homocoupling-free pgBTTT has a molar mass similar to the chloroform fraction of conventional pgBTTT (compare Figure S7 and S14), making them more comparable

https://doi.org/10.1021/jacs.5c19024
J. Am. Chem. Soc. 2026, 148, 8383−8392

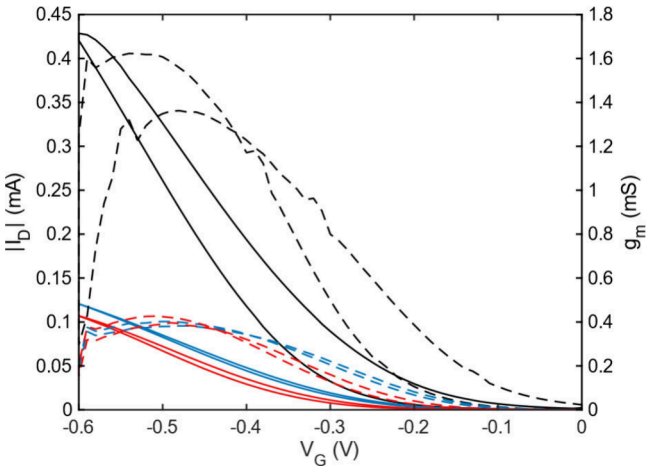

Figure 4. Transfer curves (I_D vs V_G with V_D = −0.1 V, solid lines) and voltage dependent transconductance (g_m, dashed lines) for OECT devices prepared from homocoupling-free pgBTTT (black), conventional pgBTTT (blue), and lower molar mass homocoupling-free pgBTTT (DCM fraction) (red), with channel dimensions W = 100 μm and L = 200 μm.

as OECT channel materials. An intermediate μC^* of 1390 ± 80 F cm^{-1} V^{-1} s^{-1} was observed for this DCM fraction, indicating that when polymers of similar molar mass are compared, the homocoupling-free polymer still outperforms conventional pgBTTT. These findings imply that the removal of homocoupling defects contributes to enhanced OECT performance, but that the increased molar mass, accessed through the symmetric polymerization route, is the predominant factor governing the observed improvement.[35,38,52−55] The combined effects of removing homocoupling and increasing molar mass amount to a total μC^* enhancement of 89%. All three materials show comparable operational stability during cycling measurements (100 cycles), with changes in I_D and g_m on the order of ± 10% over the cycling period for all devices (Figure S25).

It is important to note here that both conventional and homocoupling-free pgBTTT were synthesized under identical reaction conditions, demonstrating the superiority of the symmetric Stille polymerization in producing homocoupling-free polymers with high molar mass. To further confirm the robustness of this method, its reproducibility was tested by synthesizing two additional batches of homocoupling-free pgBTTT, which were also evaluated in OECTs (Table 1). In both cases, similar μC^* values were achieved, reinforcing the reliability of this new approach in producing high-performance OECT channel materials.

To determine if the enhanced performance originates from an improved electronic (hole) transport (μ) or from an increased uptake of ions (C^*), both figures of merit were also measured independently. Electrochemical impedance spectroscopy (EIS) was used to determine C^* at doping potentials of 0.4 and 0.5 V (Figure S27−S31). All polymers exhibit similar C^* values around 200 F cm^{-3}. The observed differences in the μC^* product can thus mainly be attributed to an increase of the charge carrier mobility for homocoupling-free pgBTTT. This was confirmed by measuring the electronic charge carrier transit time while pulsing constant gate current to extract the μ

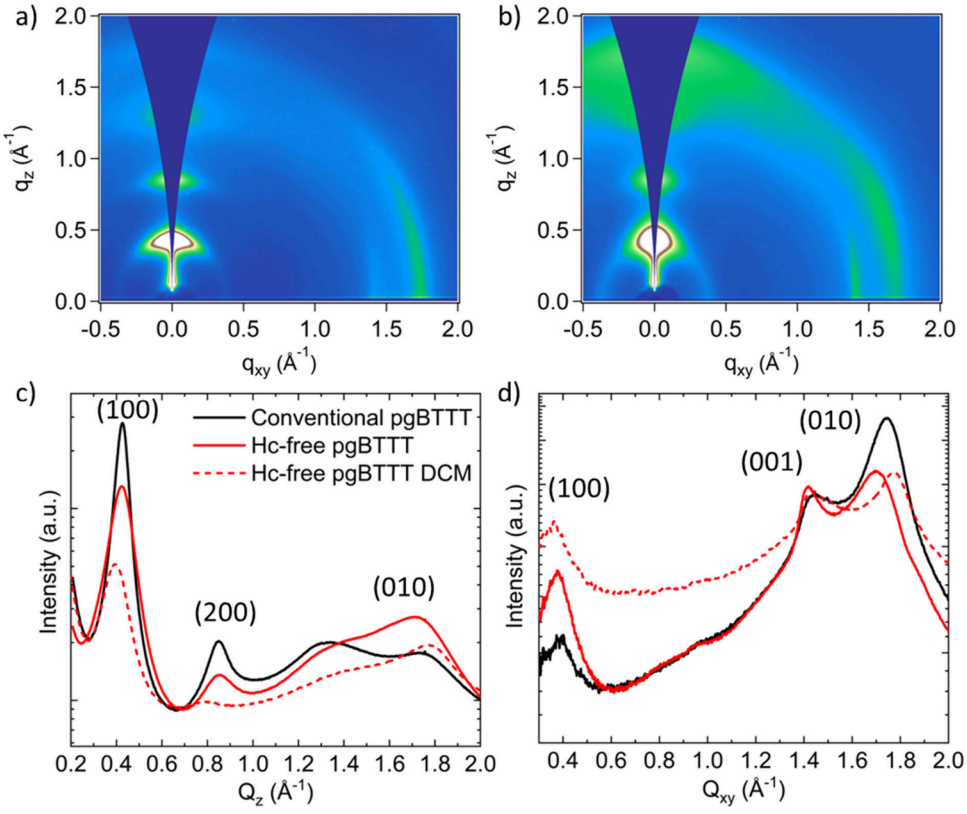

Figure 5. Two-dimensional GIWAXS patterns for a) conventional and b) (high molar mass) homocoupling-free pgBTTT. c) In-plane (Q_z) and d) out-of-plane (Q_{xy}) thickness-normalized lineouts for conventional and homocoupling-free pgBTTT. Dashed and continuous lines indicate the medium molar mass dichloromethane and the high molar mass chloroform fraction, respectively.

https://doi.org/10.1021/jacs.5c19024
J. Am. Chem. Soc. 2026, 148, 8383−8392

values (Figure S26, Table S6). It was found that the combination of a perfectly alternating backbone structure and increased molar mass amounts to an average 3-fold enhancement of μ for pgBTTT.[38,39,56]

By measuring μ and C^* separately, a comparison could be made between μC^*, derived from the OECT transfer curve, and $\mu \times C^*$, calculated by multiplying the independently measured values (Table 1, Figure S23). As shown in Table 1, a significant discrepancy was observed between the absolute values of these metrics for conventional pgBTTT and for the DCM fraction of hc-free pgBTTT. Notably, only in high molar mass batches of hc-free pgBTTT, μC^* and $\mu \times C^*$ yielded values in reasonable agreement. Shahi et al. highlighted before that transfer curve-derived μC^* values can deviate from the actual device performance.[57] The strong agreement between μC^* and $\mu \times C^*$ for high molar mass, homocoupling-free polymers suggests that these materials yield more reliable device properties, accurately reflecting their intrinsic OECT performance characteristics. Compared to similar thiophene-based p-type channel materials operating in enhancement mode, and measured in devices of comparable dimensions, homocoupling-free pgBTTT demonstrates a record performance (Figure S24).[17,29,33,58−62] This shows that our polymerization strategy effectively unlocks previously untapped potential in these types of materials.[63]

To gain insights in the solid-state microstructure of conventional pgBTTT and the homocoupling-free polymer, 2D grazing-incidence wide-angle X-ray scattering (GIWAXS) analysis was performed on films of both materials. Based on the scattering patterns (Figure 5a,b and S32), there is some variation in crystalline texture: whereas conventional pgBTTT is predominantly edge-on, the homocoupling-free variant contains a larger population of face-on crystallites in both the high and low molar mass cases. An overview of all the observed signals can be found in Table S7. When looking at the lineouts in Figure 5c,d, two orders of lamellar stacking (h00, Q_z = 0.42 and 0.86 Å^{-1}) are clearly present in both materials, which could indicate (relatively) long-range order of the crystallites.[33] The lamellar stacking distance is in good agreement with literature, amounting to 14.97 Å, and is the same for both the conventional and homocoupling-free material. Coherence length estimates (Table S8), calculated via the Scherrer equation on the (100) lamellar stacking peak, indicate a significantly smaller coherence length for the homocoupling-free material, possibly indicative of smaller crystallites. Clearly visible in the Q_z lineout is the larger intensity of the (010) π-π stacking peak in the homocoupling-free case (Q_z = 1.72 Å^{-1}, 3.70 Å), indicating a larger portion of face-on orientation. The lower molar mass (DCM) fraction of the homocoupling-free material exhibits tighter packing (Q_z = 1.77 Å^{-1}, 3.55 Å), while conventional pgBTTT (Q_z = 1.75 Å^{-1}, 3.59 Å) shows an intermediate value. This is similarly observed for the (010) peaks in the Q_{xy} direction and seems to be molar mass dependent, with lower molar mass pgBTTT showing tighter π-π stacks. The backbone seems to be more tilted relative to the substrate in the homocoupling-free material, as evidenced by the signal appearing stronger at ≈25° relative to the Q_{xy} axis (Figure 5b). In general, the absence of homocoupling defects results in a mixed edge-on and face-on morphology and large anisotropy in the film. Together with the higher molar mass, this might allow for the occurrence of more tie-chains and stronger percolation pathways for the charges. Given the bulk conductive properties of OMIECs, this suggests a stronger 3D entangled network of polymer chains in the homocoupling-free material, which may benefit mobility.[63−65]

CONCLUSIONS

In this study, we investigated the influence of homocoupling defects and molar mass on the performance of the benchmark OECT polymer, pgBTTT. By employing a symmetric Stille polymerization, homocoupling-free polymer chains with significantly higher molar mass were obtained under identical reaction conditions. The absence of structural defects and the enhanced chain length were confirmed by complementary MALDI-ToF MS and ESD-STM analysis. Comparative OECT evaluations revealed that while the removal of homocoupling defects in itself already results in an improvement in device performance, the increase in molar mass is the main factor causing the significantly enhanced μC^* product. These findings highlight the importance of controlling both molecular precision and macromolecular properties to achieve reproducible and high-performing OECT materials.

Interestingly, detailed statistical analysis of STM images revealed no significant correlation between homocoupling defects and polymer growth, challenging the long-standing assumption that such defects inherently limit chain elongation. This assumption was likely prevalent due to the prior unavailability of synthetic methods capable of producing fully homocoupling-free samples, coupled with the lack of precise analytical techniques to reliably quantify defect ratios.

Our work underscores the importance of homocoupling-free synthesis, not only for ensuring structural fidelity and reproducibility, but also for enabling a clear understanding of structure−property relationships in polymeric OMIECs. While demonstrated here for a p-type system, the same design principles are also applicable to symmetric n-type materials, where defect control may be even more critical given their currently lower device performance. We therefore encourage our peers to adopt similarly well-controlled polymerization strategies to uncover the intrinsic potential of emerging OMIECs and to accelerate their translation into practical OECT applications and beyond.

ASSOCIATED CONTENT

Supporting Information

The Supporting Information is available free of charge at https://pubs.acs.org/doi/10.1021/jacs.5c19024.

General methods section, synthesis of conventional and hc-free pgBTTT (including optimization efforts for the latter), ^{1}H and ^{13}C NMR spectra, MALDI-ToF mass spectra, cyclic voltammetry measurements, ESD-STM analysis, ICP-MS measurements, OECT, mobility and EIS measurements, and GIWAXS analysis, including Schemes S1−S4, Figures S1−S32, and Tables S1−S8 (PDF)

AUTHOR INFORMATION

Corresponding Authors

Jochen Vanderspikken − *Hasselt University, Institute for Materials Research (imo-imomec), Design & Synthesis of Organic Semiconductors (DSOS), B-3500 Hasselt, Belgium; imec, imo-imomec, B-3590 Diepenbeek, Belgium;*
orcid.org/0000-0001-7059-0155;
Email: jochen.vanderspikken@uhasselt.be

https://doi.org/10.1021/jacs.5c19024
J. Am. Chem. Soc. 2026, 148, 8383−8392

Wouter Maes − *Hasselt University, Institute for Materials Research (imo-imomec), Design & Synthesis of Organic Semiconductors (DSOS), B-3500 Hasselt, Belgium; imec, imo-imomec, B-3590 Diepenbeek, Belgium;* orcid.org/0000-0001-7883-3393; Email: wouter.maes@uhasselt.be

Giovanni Costantini − *School of Chemistry, University of Birmingham, Birmingham B15 2TT, United Kingdom; School of Physics and Astronomy, University of Birmingham, Birmingham B15 2TT, United Kingdom;* orcid.org/0000-0001-7916-3440; Email: g.costantini@bham.ac.uk

Authors

Lize Bynens − *Hasselt University, Institute for Materials Research (imo-imomec), Design & Synthesis of Organic Semiconductors (DSOS), B-3500 Hasselt, Belgium; imec, imo-imomec, B-3590 Diepenbeek, Belgium*

Paola Mantegazza − *School of Chemistry, University of Birmingham, Birmingham B15 2TT, United Kingdom*

Adam Marks − *Department of Materials Science and Engineering, Stanford University, Stanford, California 94305, United States*

Yeongmin Park − *Department of Materials Science and Engineering, Stanford University, Stanford, California 94305, United States*

Arwin Goossens − *Hasselt University, Institute for Materials Research (imo-imomec), Organic Optoelectronics (OOE), B-3500 Hasselt, Belgium; imec, imo-imomec, B-3590 Diepenbeek, Belgium*

Stefania Moro − *School of Chemistry, University of Birmingham, Birmingham B15 2TT, United Kingdom;* orcid.org/0000-0001-8445-4509

Tyler J. Quill − *Department of Materials Science and Engineering, Stanford University, Stanford, California 94305, United States;* orcid.org/0000-0003-2906-0747

Garrett Lecroy − *Department of Materials Science and Engineering, Stanford University, Stanford, California 94305, United States*

Christina Cheng − *Department of Materials Science and Engineering, Stanford University, Stanford, California 94305, United States;* orcid.org/0000-0001-8258-5329

Arianna Magni − *Department of Materials Science and Engineering, Stanford University, Stanford, California 94305, United States;* orcid.org/0000-0002-9376-4522

Laurence Lutsen − *Hasselt University, Institute for Materials Research (imo-imomec), Design & Synthesis of Organic Semiconductors (DSOS), B-3500 Hasselt, Belgium; imec, imo-imomec, B-3590 Diepenbeek, Belgium*

Simon E. F. Spencer − *Department of Statistics, University of Warwick, Coventry CV4 7AL, United Kingdom*

Koen Vandewal − *Hasselt University, Institute for Materials Research (imo-imomec), Organic Optoelectronics (OOE), B-3500 Hasselt, Belgium; imec, imo-imomec, B-3590 Diepenbeek, Belgium;* orcid.org/0000-0001-5471-383X

Alberto Salleo − *Department of Materials Science and Engineering, Stanford University, Stanford, California 94305, United States*

Complete contact information is available at: https://pubs.acs.org/10.1021/jacs.5c19024

Author Contributions

◆L.B. and P.M. contributed equally to this work. The manuscript was written through contributions of all authors. All authors have given approval to the final version of the manuscript.

Notes

The authors declare no competing financial interest.

■ ACKNOWLEDGMENTS

This project received funding from the European Union's Horizon 2020 research and innovation program under grant agreement no. 964677 (MITICS). W.M., K.V., L.B., and A.G. thank the FWO Vlaanderen for financial support (WEAVE project G025922N and Ph.D. grant 1S70122N). Use of the Stanford Synchrotron Radiation Light source, SLAC National Accelerator Laboratory, is supported by the U.S. Department of Energy, Office of Science, Office of Basic Energy Sciences under Contract No. DE-AC02-76SF00515.

■ REFERENCES

(1) Liang, Z.; Neshchadin, A.; Zhang, Z.; Zhao, F.-G.; Liu, X.; Yu, L. Stille polycondensation: a multifaceted approach towards the synthesis of polymers with semiconducting properties. *Polym. Chem.* **2023**, *14* (40), 4611−4625.

(2) Lo, C. K.; Wolfe, R. M. W.; Reynolds, J. R. From Monomer to Conjugated Polymer: A Perspective on Best Practices for Synthesis. *Chem. Mater.* **2021**, *33* (13), 4842−4852.

(3) Holliday, S.; Li, Y. L.; Luscombe, C. K. Recent advances in high performance donor-acceptor polymers for organic photovoltaics. *Prog. Polym. Sci.* **2017**, *70*, 34−51.

(4) Xiong, H.; Lin, Q.; Lu, Y.; Zheng, D.; Li, Y.; Wang, S.; Xie, W.; Li, C.; Zhang, X.; Lin, Y.; Wang, Z.-X.; Shi, Q.; Marks, T. J.; Huang, H. General room-temperature Suzuki-Miyaura polymerization for organic electronics. *Nat. Mater.* **2024**, *23*, 695−702.

(5) Hendriks, K. H.; Li, W.; Heintges, G. H.; van Pruissen, G. W.; Wienk, M. M.; Janssen, R. A. Homocoupling defects in diketopyrrolopyrrole-based copolymers and their effect on photovoltaic performance. *J. Am. Chem. Soc.* **2014**, *136* (31), 11128−33.

(6) Rudenko, A. E.; Thompson, B. C. Optimization of direct arylation polymerization (DArP) through the identification and control of defects in polymer structure. *J. Polym. Sci., Part A: Polym. Chem.* **2015**, *53* (2), 135−147.

(7) Hong, W.; Chen, S.; Sun, B.; Arnould, M. A.; Meng, Y.; Li, Y. Is a polymer semiconductor having a "perfect" regular structure desirable for organic thin film transistors? *Chem. Sci.* **2015**, *6* (5), 3225−3235.

(8) Pirotte, G.; Verstappen, P.; Vanderzande, D.; Maes, W. On the "True" Structure of Push-Pull-Type Low-Bandgap Polymers for Organic Electronics. *Adv. Electron. Mater.* **2018**, *4* (10), 1700481.

(9) Smeets, S.; Liu, Q.; Vanderspikken, J.; Quill, T. J.; Gielen, S.; Lutsen, L.; Vandewal, K.; Maes, W. Structurally Pure and Reproducible Polymer Materials for High-Performance Organic Solar Cells. *Chem. Mater.* **2023**, *35* (19), 8158−8169.

(10) Pirotte, G.; Kesters, J.; Cardeynaels, T.; Verstappen, P.; D'Haen, J.; Lutsen, L.; Champagne, B.; Vanderzande, D.; Maes, W. The Impact of Acceptor-Acceptor Homocoupling on the Optoelectronic Properties and Photovoltaic Performance of PDTSQx(ff) Low Bandgap Polymers. *Macromol. Rapid Commun.* **2018**, *39* (14), 1800086.

(11) Vanderspikken, J.; Liu, Z.; Wu, X. C.; Beckers, O.; Moro, S.; Quill, T. J.; Liu, Q.; Goossens, A.; Marks, A.; Weaver, K.; Hamid, M.; Goderis, B.; Nies, E.; Lemaur, V.; Beljonne, D.; Salleo, A.; Lutsen, L.; Vandewal, K.; Van Mele, B.; Costantini, G.; Van den Brande, N.; Maes, W. On the Importance of Chemical Precision in Organic Electronics: Fullerene Intercalation in Perfectly Alternating Conjugated Polymers. *Adv. Funct. Mater.* **2023**, *33* (52), No. 2309403.

(12) Vangerven, T.; Verstappen, P.; Drijkoningen, J.; Dierckx, W.; Himmelberger, S.; Salleo, A.; Vanderzande, D.; Maes, W.; Manca, J. V. Molar Mass versus Polymer Solar Cell Performance: Highlighting

the Role of Homocouplings. *Chem. Mater.* **2015**, *27* (10), 3726−3732.
(13) Streiter, M.; Beer, D.; Meier, F.; Göhler, C.; Lienert, C.; Lombeck, F.; Sommer, M.; Deibel, C. Homocoupling Defects in a Conjugated Polymer Limit Exciton Diffusion. *Adv. Funct. Mater.* **2019**, *29* (46), No. 1903936.
(14) Lu, L.; Zheng, T.; Xu, T.; Zhao, D.; Yu, L. Mechanistic Studies of Effect of Dispersity on the Photovoltaic Performance of PTB7 Polymer Solar Cells. *Chem. Mater.* **2015**, *27* (2), 537−543.
(15) Rivnay, J.; Inal, S.; Salleo, A.; Owens, R. M.; Berggren, M.; Malliaras, G. G. Organic electrochemical transistors. *Nat. Rev. Mater.* **2018**, *3* (2), 17086.
(16) Torricelli, F.; Adrahtas, D. Z.; Bao, Z.; Berggren, M.; Biscarini, F.; Bonfiglio, A.; Bortolotti, C. A.; Frisbie, C. D.; Macchia, E.; Malliaras, G. G.; McCulloch, I.; Moser, M.; Nguyen, T. Q.; Owens, R. M.; Salleo, A.; Spanu, A.; Torsi, L. Electrolyte-gated transistors for enhanced performance bioelectronics. *Nat. Rev. Methods Primers* **2021**, *1* (1), 66.
(17) Giovannitti, A.; Sbircea, D. T.; Inal, S.; Nielsen, C. B.; Bandiello, E.; Hanifi, D. A.; Sessolo, M.; Malliaras, G. G.; McCulloch, I.; Rivnay, J. Controlling the mode of operation of organic transistors through side-chain engineering. *Proc. Natl. Acad. Sci. U.S.A.* **2016**, *113* (43), 12017−12022.
(18) Wang, Y.; Wustoni, S.; Surgailis, J.; Zhong, Y.; Koklu, A.; Inal, S. Designing organic mixed conductors for electrochemical transistor applications. *Nat. Rev. Mater.* **2024**, *9*, 249−265.
(19) Marks, A.; Griggs, S.; Gasparini, N.; Moser, M. Organic Electrochemical Transistors: An Emerging Technology for Biosensing. *Adv. Mater. Interfaces* **2022**, *9* (6), No. 2102039.
(20) Kim, H.; Won, Y.; Song, H. W.; Kwon, Y.; Jun, M.; Oh, J. H. Organic Mixed Ionic-Electronic Conductors for Bioelectronic Sensors: Materials and Operation Mechanisms. *Adv. Sci.* **2024**, *11*, No. 2306191.
(21) Moser, M.; Ponder, J. F.; Wadsworth, A.; Giovannitti, A.; McCulloch, I. Materials in Organic Electrochemical Transistors for Bioelectronic Applications: Past, Present, and Future. *Adv. Funct. Mater.* **2019**, *29* (21), No. 1807033.
(22) He, Y.; Kukhta, N. A.; Marks, A.; Luscombe, C. K. The effect of side chain engineering on conjugated polymers in organic electrochemical transistors for bioelectronic applications. *J. Mater. Chem. C* **2022**, *10* (7), 2314−2332.
(23) Heo, S.; Kwon, J.; Sung, M.; Lee, S.; Cho, Y.; Jung, H.; You, I.; Yang, C.; Lee, J.; Noh, Y. Y. Large Transconductance of Electrochemical Transistors Based on Fluorinated Donor-Acceptor Conjugated Polymers. *ACS Appl. Mater. Interfaces* **2023**, *15* (1), 1629−1638.
(24) Savva, A.; Hallani, R.; Cendra, C.; Surgailis, J.; Hidalgo, T. C.; Wustoni, S.; Sheelamanthula, R.; Chen, X.; Kirkus, M.; Giovannitti, A.; Salleo, A.; McCulloch, I.; Inal, S. Balancing Ionic and Electronic Conduction for High-Performance Organic Electrochemical Transistors. *Adv. Funct. Mater.* **2020**, *30* (11), No. 1907657.
(25) DiTullio, B. T.; Savagian, L. R.; Bardagot, O.; De Keersmaecker, M.; Osterholm, A. M.; Banerji, N.; Reynolds, J. R. Effects of Side-Chain Length and Functionality on Polar Poly(dioxythiophene)s for Saline-Based Organic Electrochemical Transistors. *J. Am. Chem. Soc.* **2023**, *145* (1), 122−134.
(26) Heimfarth, D.; Balci Leinen, M.; Klein, P.; Allard, S.; Scherf, U.; Zaumseil, J. Enhancing Electrochemical Transistors Based on Polymer-Wrapped (6,5) Carbon Nanotube Networks with Ethylene Glycol Side Chains. *ACS Appl. Mater. Interfaces* **2022**, *14* (6), 8209−8217.
(27) Pan, T.; Wu, X.; Liu, M.; Jiang, X.; Yan, C.; Li, Y.; Zhang, P.; Li, J.; Ye, G.; Zhang, Y.; Hong, W. Ambipolar Organic Bulk Heterojunction Electrochemical Transistors for High Gain Inverters. *ACS Mater. Lett.* **2026**, *8*, 171−178.
(28) Ding, R.; Zhang, X.; Luan, Y.; Peng, M.; Chen, W.; Wang, S.; Su, S.; Lu, S.; Jeong, S. Y.; Woo, H. Y.; Guo, X.; Feng, K.; Guo, Z.-H. Donor Engineering for High Performance n-Type OECT Materials with Exceptional Operational Stability. *Angew. Chem., Int. Ed.* **2025**, *64*, No. e202513182.
(29) Moser, M.; Savagian, L. R.; Savva, A.; Matta, M.; Ponder, J. F.; Hidalgo, T. C.; Ohayon, D.; Hallani, R.; Reisjalali, M.; Troisi, A.; Wadsworth, A.; Reynolds, J. R.; Inal, S.; McCulloch, I. Ethylene Glycol-Based Side Chain Length Engineering in Polythiophenes and its Impact on Organic Electrochemical Transistor Performance. *Chem. Mater.* **2020**, *32* (15), 6618−6628.
(30) Quill, T. J.; LeCroy, G.; Halat, D. M.; Sheelamanthula, R.; Marks, A.; Grundy, L. S.; McCulloch, I.; Reimer, J. A.; Balsara, N. P.; Giovannitti, A.; Salleo, A.; Takacs, C. J. An ordered, self-assembled nanocomposite with efficient electronic and ionic transport. *Nat. Mater.* **2023**, *22* (3), 362−368.
(31) Quill, T. J.; LeCroy, G.; Marks, A.; Hesse, S. A.; Thiburce, Q.; McCulloch, I.; Tassone, C. J.; Takacs, C. J.; Giovannitti, A.; Salleo, A. Charge Carrier Induced Structural Ordering And Disordering in Organic Mixed Ionic Electronic Conductors. *Adv. Mater.* **2024**, *36*, No. e2310157.
(32) Siemons, N.; Pearce, D.; Yu, H.; Tuladhar, S. M.; LeCroy, G. S.; Sheelamanthula, R.; Hallani, R. K.; Salleo, A.; McCulloch, I.; Giovannitti, A.; Frost, J. M.; Nelson, J. Controlling swelling in mixed transport polymers through alkyl side-chain physical cross-linking. *Proc. Natl. Acad. Sci. U.S.A.* **2023**, *120* (35), No. e2306272120.
(33) Hallani, R. K.; Paulsen, B. D.; Petty, A. J.; Sheelamanthula, R.; Moser, M.; Thorley, K. J.; Sohn, W.; Rashid, R. B.; Savva, A.; Moro, S.; Parker, J. P.; Drury, O.; Alsufyani, M.; Neophytou, M.; Kosco, J.; Inal, S.; Costantini, G.; Rivnay, J.; McCulloch, I. Regiochemistry-Driven Organic Electrochemical Transistor Performance Enhancement in Ethylene Glycol-Functionalized Polythiophenes. *J. Am. Chem. Soc.* **2021**, *143* (29), 11007−11018.
(34) Liu, Z.; Vanderspikken, J.; Mantegazza, P.; Moro, S.; Hamid, M.; Mertens, S.; Van den Brande, N.; Lutsen, L.; Lemaur, V.; Beljonne, D.; Costantini, G.; Vandewal, K.; Van Mele, B.; Maes, W.; Goderis, B. Removing Homocoupling Defects in Alkoxy/Alkyl-PBTTT Enhances Polymer:Fullerene Co-Crystal Formation and Stability. *Adv. Funct. Mater.* **2024**, No. 2413647.
(35) Wu, H. Y.; Yang, C. Y.; Li, Q.; Kolhe, N. B.; Strakosas, X.; Stoeckel, M. A.; Wu, Z.; Jin, W.; Savvakis, M.; Kroon, R.; Tu, D.; Woo, H. Y.; Berggren, M.; Jenekhe, S. A.; Fabiano, S. Influence of Molecular Weight on the Organic Electrochemical Transistor Performance of Ladder-Type Conjugated Polymers. *Adv. Mater.* **2022**, *34* (4), No. e2106235.
(36) Lo, C. Y.; Wu, Y.; Awuyah, E.; Meli, D.; Nguyen, D. M.; Wu, R.; Xu, B.; Strzalka, J.; Rivnay, J.; Martin, D. C.; Kayser, L. V. Influence of the molecular weight and size distribution of PSS on mixed ionic-electronic transport in PEDOT:PSS. *Polym. Chem.* **2022**, *13* (19), 2764−2775.
(37) Dai, Y.; Dai, S.; Li, N.; Li, Y.; Moser, M.; Strzalka, J.; Prominski, A.; Liu, Y.; Zhang, Q.; Li, S.; Hu, H.; Liu, W.; Chatterji, S.; Cheng, P.; Tian, B.; McCulloch, I.; Xu, J.; Wang, S. Stretchable Redox-Active Semiconducting Polymers for High-Performance Organic Electrochemical Transistors. *Adv. Mater.* **2022**, *34* (23), No. e2201178.
(38) Tropp, J.; Meli, D.; Wu, R.; Xu, B.; Hunt, S. B.; Azoulay, J. D.; Paulsen, B. D.; Rivnay, J. Revealing the Impact of Molecular Weight on Mixed Conduction in Glycolated Polythiophenes through Electrolyte Choice. *ACS Mater. Lett.* **2023**, *5* (5), 1367−1375.
(39) Chae, S.; Nguyen-Dang, T.; Chatsirisupachai, J.; Yi, A.; Vázquez, R. J.; Quek, G.; Promarak, V.; Kim, H. J.; Bazan, G. C.; Nguyen, T. Q. Impact of Molecular Weight on the Ionic and Electronic Transport of Self-Doped Conjugated Polyelectrolytes Relevant to Organic Electrochemical Transistors. *Adv. Funct. Mater.* **2024**, *34* (3), No. 2310852.
(40) Ansari, M. A.; Mohiuddin, S.; Kandemirli, F.; Malik, M. I. Synthesis and characterization of poly(3-hexylthiophene): improvement of regioregularity and energy band gap. *RSC Adv.* **2018**, *8*, 8319−8328.
(41) Ong, B. S.; Wu, Y.; Liu, P.; Gardner, S. High-Performance Semiconducting Polythiophenes for Organic Thin-Film Transistors. *J. Am. Chem. Soc.* **2004**, *126* (11), 3378−3379.

https://doi.org/10.1021/jacs.5c19024
J. Am. Chem. Soc. 2026, 148, 8383−8392

(42) Pan, H.; Li, Y.; Wu, Y.; Liu, P.; Ong, B. S.; Zhu, S.; Xu, G. Low-Temperature, Solution-Processed, High-Mobility Polymer Semiconductors for Thin-Film Transistors. *J. Am. Chem. Soc.* **2007**, *129* (14), 4112−4113.
(43) Moro, S.; Siemons, N.; Drury, O.; Warr, D. A.; Moriarty, T. A.; Perdigao, L. M. A.; Pearce, D.; Moser, M.; Hallani, R. K.; Parker, J.; McCulloch, I.; Frost, J. M.; Nelson, J.; Costantini, G. The Effect of Glycol Side Chains on the Assembly and Microstructure of Conjugated Polymers. *ACS Nano* **2022**, *16* (12), 21303−21314.
(44) Moro, S.; Spencer, S. E. F.; Lester, D. W.; Nubling, F.; Sommer, M.; Costantini, G. Molecular-Scale Imaging Enables Direct Visualization of Molecular Defects and Chain Structure of Conjugated Polymers. *ACS Nano* **2024**, *18* (18), 11655−11664.
(45) Warr, D. A.; Perdigao, L. M. A.; Pinfold, H.; Blohm, J.; Stringer, D.; Leventis, A.; Bronstein, H.; Troisi, A.; Costantini, G. Sequencing conjugated polymers by eye. *Sci. Adv.* **2018**, *4* (6), eaas9543.
(46) Ponder, J. F., Jr; Chen, H.; Luci, A. M. T.; Moro, S.; Turano, M.; Hobson, A. L.; Collier, G. S.; Perdigão, L. M. A.; Moser, M.; Zhang, W.; Costantini, G.; Reynolds, J. R.; McCulloch, I. Low-Defect, High Molecular Weight Indacenodithiophene (IDT) Polymers Via a C−H Activation: Evaluation of a Simpler and Greener Approach to Organic Electronic Materials. *ACS Mater. Lett.* **2021**, *3*, 1503−1512.
(47) Wu, X.; Moro, S.; Marks, A.; Alsufyani, M.; Yu, Z.; Perdigão, L. M. A.; Chen, X.; Luci, A. M. T.; Crockford, C.; Spencer, S. E. F.; Fox, D. J.; Pei, J.; McCulloch, I.; Costantini, G. Revealing polymerization defects and formation mechanisms in aldol condensation for conjugated polymers via high-resolution molecular imaging. *Nat. Commun.* **2025**, *16*, 7031.
(48) Moser, M.; Savva, A.; Thorley, K.; Paulsen, B. D.; Hidalgo, T. C.; Ohayon, D.; Chen, H.; Giovannitti, A.; Marks, A.; Gasparini, N.; Wadsworth, A.; Rivnay, J.; Inal, S.; McCulloch, I. Polaron Delocalization in Donor-Acceptor Polymers and its Impact on Organic Electrochemical Transistor Performance. *Angew. Chem., Int. Ed. Engl.* **2021**, *60* (14), 7777−7785.
(49) Jia, H.; Huang, Z.; Li, P.; Zhang, S.; Wang, Y.; Wang, J.-Y.; Gu, X.; Lei, T. Engineering donor−acceptor conjugated polymers for high-performance and fast-response organic electrochemical transistors. *J. Mater. Chem. C* **2021**, *9* (14), 4927−4934.
(50) Giovannitti, A.; Maria, I. P.; Hanifi, D.; Donahue, M. J.; Bryant, D.; Barth, K. J.; Makdah, B. E.; Savva, A.; Moia, D.; Zetek, M.; Barnes, P. R. F.; Reid, O. G.; Inal, S.; Rumbles, G.; Malliaras, G. G.; Nelson, J.; Rivnay, J.; McCulloch, I. The Role of the Side Chain on the Performance of N-type Conjugated Polymers in Aqueous Electrolytes. *Chem. Mater.* **2018**, *30* (9), 2945−2953.
(51) Vanderspikken, J.; Verstappen, P.; Maes, W. Extracting Structural Data from MALDI-ToF Mass Spectrometry Analysis of Alternating Conjugated Polymers - A Case Study on PBTTT Derivatives. *Macromolecules* **2024**, *57* (15), 7138−7155.
(52) Kline, R. J.; McGehee, M. D.; Kadnikova, E. N.; Liu, J.; Fréchet, J. M. J. Controlling the Field-Effect Mobility of Regioregular Polythiophene by Changing the Molecular Weight. *Adv. Mater.* **2003**, *15* (18), 1519−1522.
(53) Kline, R. J.; McGehee, M. D.; Kadnikova, E. N.; Liu, J.; Fréchet, J. M. J.; Toney, M. F. Dependence of Regioregular Poly(3-hexylthiophene) Film Morphology and Field-Effect Mobility on Molecular Weight. *Macromolecules* **2005**, *38* (8), 3312−3319.
(54) Tripathi, A. S. M.; Sadakata, S.; Gupta, R. K.; Nagamatsu, S.; Ando, Y.; Pandey, S. S. Implication of Molecular Weight on Optical and Charge Transport Anisotropy in PQT-C12 Films Fabricated by Dynamic FTM. *ACS Appl. Mater. Interfaces* **2019**, *11* (31), 28088−28095.
(55) Tran, D. K.; Robitaille, A.; Hai, I. J.; Lin, C.-C.; Kuzuhara, D.; Koganezawa, T.; Chiu, Y.-C.; Leclerc, M.; Jenekhe, S. A. Unified Understanding of Molecular Weight Dependence of Electron Transport in Naphthalene Diimide-Based n-Type Semiconducting Polymers. *Chem. Mater.* **2022**, *34* (21), 9644−9655.
(56) Ma, B.; Shi, Q.; Ma, X.; Li, Y.; Chen, H.; Wen, K.; Zhao, R.; Zhang, F.; Lin, Y.; Wang, Z.; Huang, H. Defect-Free Alternating Conjugated Polymers Enabled by Room-Temperature Stille Polymerization. *Angew. Chem., Int. Ed. Engl.* **2022**, *61* (16), No. e202115969.
(57) Shahi, M.; Le, V. N.; Alarcon Espejo, P.; Alsufyani, M.; Kousseff, C. J.; McCulloch, I.; Paterson, A. F. The organic electrochemical transistor conundrum when reporting a mixed ionic-electronic transport figure of merit. *Nat. Mater.* **2024**, *23* (1), 2−8.
(58) Schmode, P.; Savva, A.; Kahl, R.; Ohayon, D.; Meichsner, F.; Dolynchuk, O.; Thurn-Albrecht, T.; Inal, S.; Thelakkat, M. The Key Role of Side Chain Linkage in Structure Formation and Mixed Conduction of Ethylene Glycol Substituted Polythiophenes. *ACS Appl. Mater. Interfaces* **2020**, *12* (11), 13029−13039.
(59) Moser, M.; Hidalgo, T. C.; Surgailis, J.; Gladisch, J.; Ghosh, S.; Sheelamanthula, R.; Thiburce, Q.; Giovannitti, A.; Salleo, A.; Gasparini, N.; Wadsworth, A.; Zozoulenko, I.; Berggren, M.; Stavrinidou, E.; Inal, S.; McCulloch, I. Side Chain Redistribution as a Strategy to Boost Organic Electrochemical Transistor Performance and Stability. *Adv. Mater.* **2020**, *32* (37), No. e2002748.
(60) Moser, M.; Wang, Y.; Hidalgo, T. C.; Liao, H.; Yu, Y.; Chen, J.; Duan, J.; Moruzzi, F.; Griggs, S.; Marks, A.; Gasparini, N.; Wadsworth, A.; Inal, S.; McCulloch, I.; Yue, W. Propylene and butylene glycol: new alternatives to ethylene glycol in conjugated polymers for bioelectronic applications. *Mater. Horiz.* **2022**, *9*, 973−980.
(61) Chen, S. E.; Flagg, L. Q.; Onorato, J. W.; Richter, L. J.; Guo, J.; Luscombe, C. K.; Ginger, D. S. Impact of varying side chain structure on organic electrochemical transistor performance: a series of oligoethylene glycol-substituted polythiophenes. *J. Mater. Chem. A* **2022**, *10* (19), 10738−10749.
(62) Tseng, H.-S.; Puangniyom, T.; Chang, C.-Y.; Janardhanan, J. A.; Yu, H.-h.; Chen, W.-C.; Chueh, C.-C.; Hsiao, Y.-S. Strategically tailoring ethylene glycol side chains with bridged-carbonyl ester in polythiophene-based organic electrochemical transistors for bioelectronics. *J. Chem. Eng.* **2024**, *486*, No. 150371.
(63) Tropp, J.; Meli, D.; Rivnay, J. Organic mixed conductors for electrochemical transistors. *Matter* **2023**, *6* (10), 3132−3164.
(64) Fratini, S.; Nikolka, M.; Salleo, A.; Schweicher, G.; Sirringhaus, H. Charge transport in high-mobility conjugated polymers and molecular semiconductors. *Nat. Mater.* **2020**, *19* (5), 491−502.
(65) LeCroy, G.; Ghosh, R.; Sommerville, P.; Burke, C.; Makki, H.; Rozylowicz, K.; Cheng, C.; Weber, M.; Khelifi, W.; Stingelin, N.; Troisi, A.; Luscombe, C.; Spano, F. C.; Salleo, A. Using Molecular Structure to Tune Intrachain and Interchain Charge Transport in Indacenodithiophene-Based Copolymers. *J. Am. Chem. Soc.* **2024**, *146* (31), 21778−21790.

https://doi.org/10.1021/jacs.5c19024
J. Am. Chem. Soc. 2026, 148, 8383−8392